# COAL MINE SEISMICITY AND BUMPS: HISTORICAL CASE STUDIES AND CURRENT FIELD ACTIVITY

**John L. Ellenberger**, *Mining Engineer*
**Keith A. Heasley**, *Supervisory Physical Scientist*
National Institute for Occupational Safety and Health
Pittsburgh Research Laboratory
Pittsburgh, PA

## ABSTRACT

The National Institute for Occupational Safety and Health (NIOSH) has continued the research role of the former U.S. Bureau of Mines to develop techniques that will reduce the hazards in the mining work place associated with coal bumps. Current research focuses on both analyzing historical seismic data from bump-prone operations and utilizing a mine-wide seismic network to investigate the exact strata failure mechanics associated with bump-prone geology. The anticipated outcome of this research will be reduced bump incidences through advanced engineering concepts and designs which implement the new understanding of strata behavior.

The analysis of the historic seismic data consists of correlating observed mining seismicity with the geologic and geometric parameters at the sites. The primary seismic parameters are the timing, location and magnitude of a recorded seismic event. These parameters are correlated with such mining parameters as: the overburden, the size of the immediate gob, the size of the district gob area, etc. This detailed analysis of historical seismic data has provided an informative quantifiable relationship between many of the specific mining parameters and the induced seismicity.

The second aspect of the coal bump research is the instrumentation of an appropriate field site to determine the main roof, floor, and gob behavior associated with bump behavior. The chosen field site is a deep-cover longwall mine with competent geology in a historically bump-prone area. The primary field instrumentation is a three-dimensional, full-waveform, seismic array with both surface and underground sensors surrounding an active multi-panel district. The purpose of this seismic array is to determine the timing, the exact location, and the mechanism (tensile fracture, bedding plane slip, etc.) of the failure of the strata surrounding the active and multi-panel gobs. The preliminary results presented in this paper help to define the strata failure areas around the longwall panel.

### INTRODUCTION

Coal mine bumps, sometimes referred to as outbursts, bursts, or bounces, have been recognized as a serious problem in mining for more than 75 years. For the purposes of this paper, a bump is defined as a sudden release of geologic strain energy that results in the expulsion of coal from a rib or pillar in a catastrophic manner. Beginning as early as the 1930's, the U.S. Bureau of Mines conducted research relating to causes and potential mechanism to avoid bumps in coal mines (*1*). Current research being conducted by the National Institute for Occupational Safety and Health (NIOSH) remains focused on the reduction and elimination of bumps.

In the past, bumps have been acknowledged as having a greater likelihood of occurrence at depths greater than 300 m (1,000 ft), in the presence of strong roof and/or floor, and when an unusually strong massive unit exists in the main roof (*1, 2, 3*). Miners working under one or more of these conditions need to be constantly aware of the possibility of a coal bump. Recently, the U.S. coal industry experienced several consecutive years with no fatal accidents resulting from bumps, until November of 1996, when three fatalities and five additional serious injuries occurred in a two week period.

Coal bumps are often associated with seismic events that are large enough to be registered by regional seismic networks. However, not every potentially hazardous bump generates a regional seismic event, nor does every mine-induced, regional seismic event manifest itself as a coal outburst at the seam level. In reality, coal bumps are just one subset of mine-induced seismicity, and like mine-induced non-bump events, they can exhibit a wide range of magnitudes and energy release. But, knowing that coal bumps are a subset of mine seismicity, it seems reasonable that analyzing mine seismicity in general may provide a better understanding of the causes and control of mine bumps. Also, there are considerably more documented mine-induced, non-bump, seismic events than there are documented coal bumps. In fact, the seismic network in Utah has found the most active seismic area since 1962 to be the vicinity of the active coal mining with hundreds of mining-induced events recorded each year (*4*). With this number of

events, it would seem possible to develop statistically significant relationships between mining parameters and the occurrence of the mine-induced seismic events that would not be evident using the much smaller subset of actual coal bumps.

This paper presents a correlation analysis between the observed mining-induced seismicity and the geologic and geometric parameters at bump-prone sites. The analysis provides a number of results which support previous research and a number of results which may question conventional wisdom. The paper also presents some of the preliminary results from a recent three-dimensional seismic system installed at a bump-prone site.

## CASE STUDY A

The first seismic study location, Site A, operates in a coalbed varying from 2.4 to 3.6 m (8.0 to 12.0 ft) in thickness. The immediate roof varies, generally consisting of a laminated gray shale; however, in places, the immediate or main roof varies from a weak, highly fossilized and slickensided black shale to a strong siltstone, or sometimes, a sandstone channel system.

This mine progressed through 10 longwall panels without incident, then encountered bumps related to increasing depth and a sandstone channel system that resulted in abrupt changes in the physical characteristics of the immediate roof. In the following longwall district, multiple-seam interactions in conjunction with sandstone channels appeared to manifest coal bumps (*3*). Information in this current report covers the bumps encountered in the final longwall district of the mine where neither sandstone channels nor multiple-seam mining was evident.

At least six different gate road designs were utilized at Site A. The coal pillar configuration historically used was a three-entry yield-abutment design, later being changed to a four-entry yield-abutment-yield design. Pillar dimensions frequently varied from one gate road to the next. However, all the three-entry systems were configured similarly, with the abutment pillar placed adjacent to the longwall panel in the headgate. In the earlier three-entry designs, the dimensions of both pillars were increased in successive designs, to account for increasing overburden (*3*). In the current report, the pillar design was consistent across the study area, and had evolved to a four-entry, yield-abutment-yield configuration (figure 1). Topographic relief varied sharply across the panels included in this study, varying from 150 to 660 m (500 to 2,200 ft).

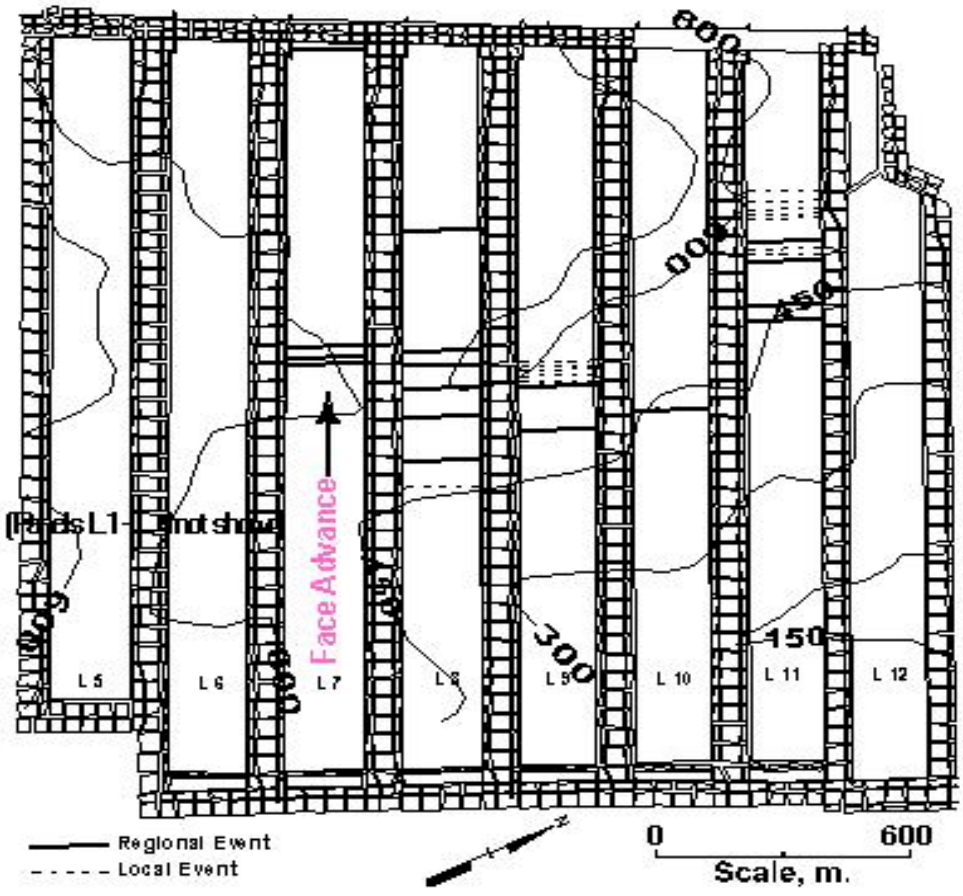


Figure 1. Panel and face locations of regional and Local events at Mine A

Bump/Seismic Events

Figure 1 shows the face locations at the time when the mine records listed 48 different events (the figure shows less than 48 face positions because, on several occasions, more than one event occurred in one day). These events were initially recorded on the foreman's reports because coal was ejected from the face and/or large vibrations were felt from the tailgate/gob area. A large number of theses events appear to have been smaller local events where some coal was ejected from the face, but no large ground vibrations were evident. On the other hand, 22 of these bump/seismic events registered a magnitude of 2.8 or greater on regional seismic monitoring networks. These 22 regional seismic events and the mine parameters at the time of the event are presented in table 1. Analyzing this small database of mine-induced seismic events produced a number of notable correlations.

**Effect of Overburden on Mine Seismicity**

Deep cover and/or strong lithologic units have long been recognized as necessary contributors to coal bumps (*1*). With this in mind, the distribution of the seismic events from Site A with respect to overburden was produced as shown in figure 2. (In order to normalize the number of seismic events occurring at a particular overburden range with relation to the amount of panel that was mined at that overburden range, the "event rate" was determined as the number of events that occurred per 300 m (1,000 ft) of panel advance at that overburden. For example, 5 events occurring in 2,200 m (7,200 ft) of face advance under overburden ranging from 300 to 375 m (1,000 to 1,250 ft), would produce an event rate of 0.69 (5/7.2) per 300 m (1,000 ft).) Clearly, the seismic events at this site are biased towards the deeper cover. In particular, all of the events occurred when the overburden was greater than 500 m (1,625 ft) although over one-third of the extraction area was under less than this amount of cover.

Table 1. Summary of Bump/Seismic Events.

| Date | Intensity (UK, VPI)[1] | Overburden, m | Panel | Distance to max. overburden, m | Side distance to solid from tailgate, m | Distance to setup room, m | Distance to recovery room, m | ALPS stability factor | Distance to first solid, m | Energy (UK, VPI)[1] |
|---|---|---|---|---|---|---|---|---|---|---|
| 7/31/1994 | 3 | 738 | L-7 | 0 | 1402 | 1144 | 822 | 0.58 | 822 | 925 |
| 8/1/1994 | 3 | 738 | L-7 | -34 | 1402 | 1163 | 803 | 0.58 | 803 | 925 |
| 8/3/1994 | 3.5 | 738 | L-7 | -46 | 1402 | 1193 | 773 | 0.58 | 773 | 2465 |
| 10/5/1994 | 3.6 | 731 | L-7 | -823 | 1402 | 1954 | 12 | 0.58 | 12 | 2998 |
| 12/23/1994 | N/A, 3.5 | 592 | L-8 | 186 | 1676 | 869 | 1097 | 0.74 | 869 | n/a, 2465 |
| 1/12/1995 | 3.5 | 661 | L-8 | 46 | 1676 | 1013 | 953 | 0.65 | 953 | 2465 |
| 1/12/1995 | 3 | 661 | L-8 | 46 | 1676 | 1013 | 953 | 0.65 | 953 | 925 |
| 1/12/1995 | 3 | 661 | L-8 | 46 | 1676 | 1013 | 953 | 0.65 | 953 | 925 |
| 1/19/1995 | 3.7 | 679 | L-8 | -24 | 1676 | 1085 | 881 | 0.63 | 881 | 3648 |
| 1/30/1995 | 3.7 | 687 | L-8 | -107 | 1676 | 1149 | 817 | 0.62 | 817 | 3648 |
| 2/4/1995 | 2.8, 3.3 | 668 | L-8 | -140 | 1676 | 1205 | 761 | 0.65 | 761 | 625, 1665 |
| 2/4/1995 | 2.8, 3.3 | 668 | L-8 | -140 | 1676 | 1205 | 761 | 0.65 | 761 | 625, 1665 |
| 3/11/1995 | 4 | 592 | L-8 | -472 | 1676 | 1527 | 439 | 0.74 | 439 | 6568 |
| 3/11/1995 | 3.4 | 592 | L-8 | -472 | 1676 | 1527 | 439 | 0.74 | 439 | 2026 |
| 7/22/1995 | 2.9, 2.9 | 592 | L-9 | 216 | 1951 | 968 | 998 | 0.74 | 968 | 760, 760 |
| 8/5/1995 | 2.8 | 661 | L-9 | 91 | 1951 | 1090 | 876 | 0.65 | 876 | 625 |
| 10/25/1995 | 3.4, 4.1 | 574 | L-10 | 433 | 2225 | 1003 | 963 | 0.77 | 963 | 2026, 7990 |
| 4/19/1996 | 3.7 | 566 | L-11 | 277 | 2499 | 1266 | 700 | 0.78 | 700 | 3648 |
| 5/4/1996 | 3.2, 3.7 | 609 | L-11 | 158 | 2499 | 1390 | 576 | 0.72 | 576 | 1369, 3648 |
| 5/13/1996 | 2.7, 3.5 | 653 | L-11 | 232 | 2499 | 1497 | 469 | 0.66 | 469 | 513, 2465 |
| 5/13/1996 | 2.5, 3.5 | 653 | L-11 | 232 | 2499 | 1497 | 469 | 0.66 | 469 | 347, 2465 |
| 5/16/1996 | 2 | 668 | L-11 | 107 | 2499 | 1528 | 438 | 0.65 | 438 | 130 |

[1] Seismic data were collected and compared from both the University of Kentucky (UK) and Virginia Polytechnic Institute (VPI) systems, single values representing UK data are presented first, when both stations recorded events, UK then VPI are provided. Magnitude type ($M_L$-$M_C$) is unknown.

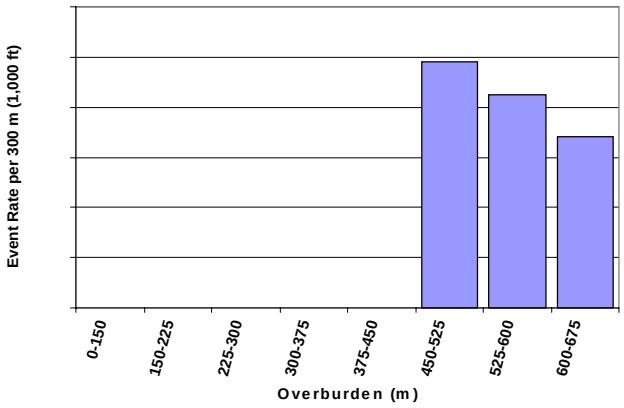


Figure 2. Event rate per 300 m (1,000 ft) vs overburden at Mine A

**Distance to Nearest Panel End**

Another observation that one may make from reviewing figure 1 is that the face had progressed through a significant portion of the panel when the seismic events occurred. Similarly, few of the seismic events occurred when the face was very close to the end of a panel. Figure 3 shows the seismic events plotted against face distance to the nearest end of the panel. With this figure and figure 1, it can be seen that no events occurred during the first 900 m (3,000 ft) of face advance in any of the panels in the district. And even taking into account a number of events that occurred closer to the end of the panels, over 95 percent of the bumps occurred greater than 300 m (1,000 ft) from either end of the panels.

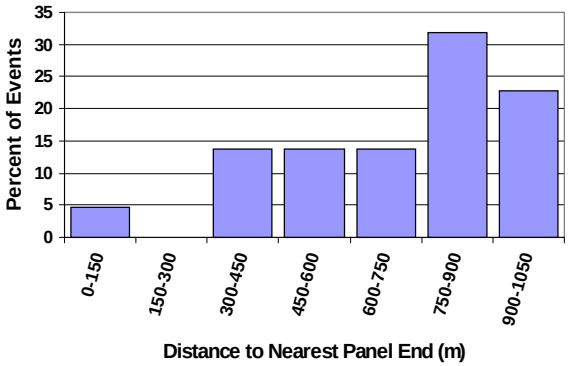


Figure 3. Distribution of events occurring at Mine A relative to the nearest panel end of the longwall panels.

**Side Distance to Solid**

In other bump-prone mines, it has been suggested that the width of the district gob (over multiple panels) has a distinct influence on the occurrence of bumps. In this paper, we refer to the total width of the district gob area, as measured from the tailgate across the adjacent gob from previous panels to the starting edge of the longwall district, as the "side distance to solid." At this site, no seismic events were observed until the distance to the side boundary of the district exceeded 1,200 m (4,000 ft) (figure 4). In fact, panels L-5 and L-6 had more overburden than panels L-7 through L-11 where the recorded bumps occurred, but the side distance to solid was only 600 and 900 m (2,000 and 3,000 ft), respectively.

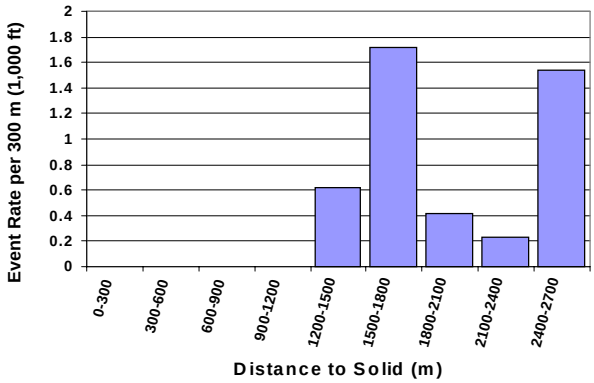


Figure 4. Event rate per 300 m (1,000 ft) vs distance to solid in meters at Mine A

**Relationship between Seismic Events and ALPS Pillar Stability**

In the past, the occurrence of bumps was shown to be related to low gateroad stability factors as calculated by the Analysis of Longwall Pillar Stability (ALPS) program (*3, 5*). (The ALPS stability factor is essentially a measure of the strength-to-load ratio of the gateroad pillar system.) In this analysis, the ALPS stability factor was correlated with the seismic activity. In order to accomplish this correlation, the overburden above each abutment pillar was measured and the ALPS stability factor was calculated. Next, factors for the individual pillars were then grouped into 75 m (250 ft) increments of overburden. Finally, the observed seismic events were associated with the ALPS stability factor of the tailgate pillar configuration for the face location at the time of the event and the results were charted as shown in figure 5. This histogram and table 1 show that the first seismic event was not encountered until the gateroad ALPS stability factor was 0.78, and that all other events occurred when the ALPS stability factor was less than 0.78. (Since the pillar design was essentially the same within the analyzed longwall district,

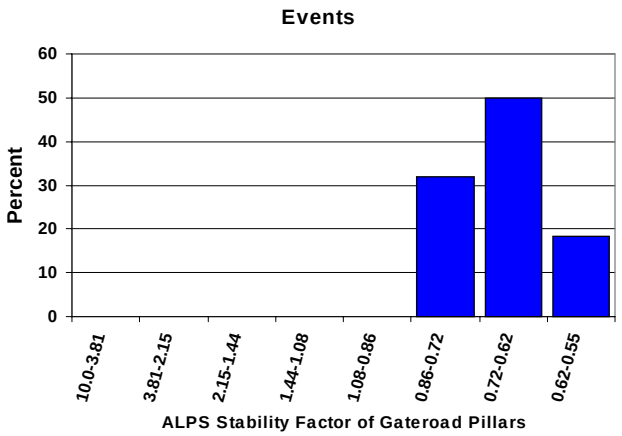


Figure 5. Percentage distribution of events by ALPS stability factor of gateroad pillars

the differences in the ALPS stability factors correlate directly to depth; therefore, the distribution in figure 5 is essentially identical to the distribution of events with respect to overburden as shown in figure 1.)

**Seismic Energy of the Events**

Up until this point in the paper, only the occurrence of an event has been analyzed and the relative size of the events has been ignored. Of course, correlating the size, or energy, of the events to the mining parameters may reveal some useful information. The regional seismic events are typically reported in Richter magnitude which is a logarithmic scale with relation to the size/energy of the event. In order to get a better perspective on the relative magnitude of these events, the logarithmic Richter magnitudes were converted to pure energy values using the following formula:

$$\log E_S = 1.96\, M_L + 9.05 \qquad (1)$$

where: $\log E_S$ = energy released (ergs) and
$M_L$ = Richter magnitude

This equation (6) has a number of assumptions built into the derivation because of the empirical nature of the Richter calculation. Therefore, the absolute energy values calculated by the equation are somewhat debatable; however, for our purposes, the calculated energy values can be considered consistent in a relative sense. For the analysis, the average energy per event and the percentage of energy released for each overburden interval was calculated. The result is presented in figure 6. In terms of energy released, it is notable that the average energy per event was highest in the events that occurred in the range of 450 to 525 m (1,500 to1,750 ft) and that average energy per event decreased at greater depths.

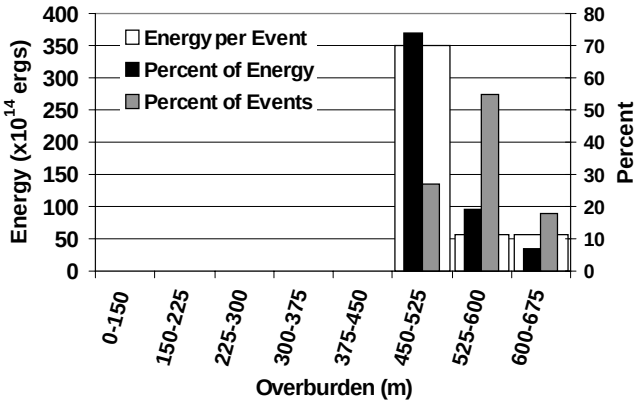


Figure 6. Distribution of energy per event, percent of energy, and percent of events at Mine A

**Discussion**

From this first look a small number of seismic events at Mine A, a number of interesting observations were presented: (1) all the bumps occurred under more than 450 m (1,500 ft) of overburden; (2) all the bumps occurred where the panel had advanced at least 900 m (3,000 ft) and the mined area was a lateral distance of greater than 1200 m (4,000 ft) to solid coal; and (3) the energy released per event did not continue to increase with increasing overburden. These observations are all informative and suggest some geometric limitations associated with the seismic events.

Some caution needs to be used when looking at these results and interpreting the individual effect of the mining parameters. Looking at figure 1, it can be seen that the deepest overburden generally occurs near the center of the longwall district. This geometry forces a strong correlation between the depth of cover and the middle of the panels. Thus some of the above results concerning the mining distance from the ends of the panels may just be a cross-correlation with depth.

## CASE STUDY B AND C

After finding some useful correlations with the limited number of seismic events available at Mine A, it was decided to continue analyzing seismic events in relation to mining parameters at a couple other mines with considerably more recorded seismic activity. These two mines have a long history of longwall mining and have each extracted numerous panels causing numerous seismic events to be registered by the regional seismic system. For our analysis, all of the regional events located within approximately a 5 km (3 mi) radius of the mines was considered to be mine-induced. (Realizing that the average horizontal location error for the regional seismic events was approximately 1.5 km (1 mi), a large area around the mines was included in order to collect all of the mining related seismic events from the regional database.) Further, to insure good quality of the event detection, only the events with a Richter magnitude of 2.0 or greater were considered. The event selection was narrowed even more by including only those events occurring within a six year period of active seismicity, this procedure resulted in 623 events associated with the two mines.

In order to perform the analysis with these mines, each monthly longwall extraction area was considered to be a separate mining sample. The center of this sample area was determined and the appropriate parameters: advance footage, overburden depth, distance from panel start, distance from panel end and side distance to solid were assigned to the area. Then, each seismic event within the month of the extraction was assigned to that sample area. This resulted in 436 events associated with Mine B and 187 events associated with Mine C.

**Event Rate Versus Overburden**

The first parameter to be examined for the properties was the event rate versus the overburden and this is plotted in figure 7. Similar to Mine A, there is very little activity until

the overburden reaches a lower limit of 375 m (1,250 ft). Also as seen at Mine A, the event rate is seen to decrease after the maximum rate around 450 m (1,500 ft) of overburden. Intuitively, the seismic event rate might be anticipated to increase with increasing overburden. The data from all three mines seems to conflict with this hypothesis. All of these mines reach a maximum event rate between 450 and 525 m (1,500 and 1,750 ft) of overburden and then the rate distinctly declines at greater depths.

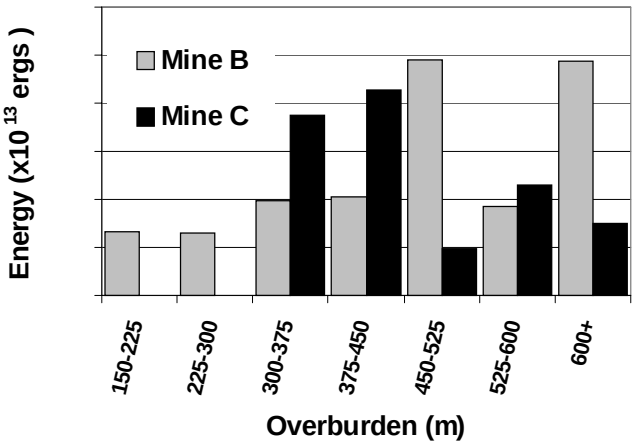


Figure 8. Average energy per event (x$10^{13}$ ergs) distributed by overburden

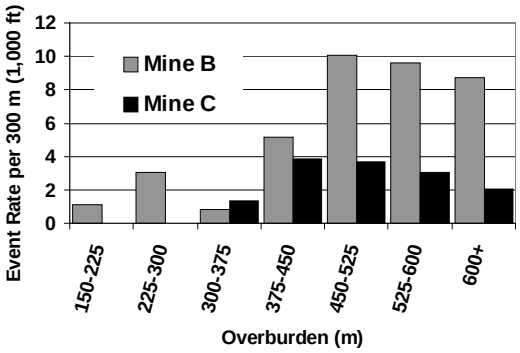


Figure 7. Event rate per 300 m (1,000 ft) versus overburden at Mines B and C

**Energy Released Versus Overburden**

The average energy per event by overburden range for Mines B and C was calculated using the same equation presented for Mine A and is plotted in figure 8. Here again, the sample does not indicate that the seismic energy continues to increase with depth as one might initially anticipate. In mine C, the highest measured average energy is encountered

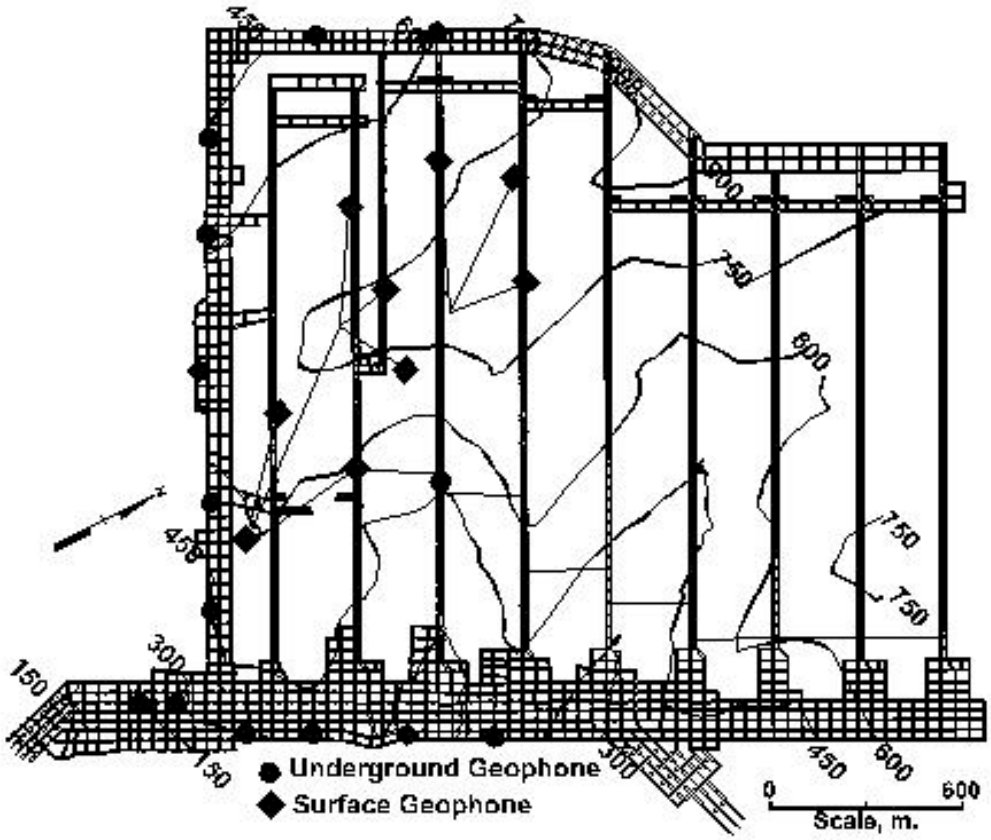


Figure 9. Mine outline showing locations of surface and undergreound geophones

when the overburden is between 300 and 450 m (1,000 and 1,500 ft), and in Mine B, the highest measured average energy occurs when overburden is in the range of 450 to 525 m (1,500 to1,750 ft). In both mines, the energy per event generally drops at greater depths (the only exception being Mine C at greater than 600 m (2,000 ft) of overburden). When this drop in the average energy per event is coupled with the drop in event rate with depth (figure 9), it can be determined that over 75 percent of the measured seismic energy occurs in the overburden range of 375 to 525 m (1,250 to 1,750 ft).

**Discussion**

This brief analysis of mine-induced seismicity has produced some interesting results. First, the seismic data clearly show that very few detectable events occur with less than 300 m (1,000 ft) of overburden, and it is not until greater than 375 to 450 m (1,250 to 1,500 ft) that the majority of seismic activity occurs. This behavior almost exactly matches the expected occurrence and depth ranges for coal bumps, and supports the possibility that reducing the overall mine seismicity will similarly reduce the bump frequency.

Second, the seismic data indicate that both the event rate and the event energy do not continue to increase with depth, but actually decrease slightly above approximately 450 m (1,500 ft) of cover. This result initially seems to be counter intuitive, but upon further thought, it is not totally unreasonable to hypothesis that the fracture processes around a longwall panel may reach a steady state, or even decline, above a certain depth. Certainly, the upper strata will have a tendency to bend versus fracturing as it becomes more remote from the extraction area. Also, the actual fracturing around the panel may become more plastic and less brittle, thereby releasing less seismic energy, with higher confinement stresses at greater depths. This aspect of the data poses some interesting questions and certainly needs to be investigated further.

## MICROSEISMIC FIELD SITE

The NIOSH project which is presently investigating bump hazards is titled; "Coal Bump Reduction through Advanced Mine Design". The basic research approach of this project is to instrument a deep, bump-prone longwall mine and determine the main roof, gob, and floor behavior using a three-dimensional, microseismic system. This microseismic system "listens" to the rock and determines the timing and location of the failure of the rock strata surrounding the longwall. By analyzing the observed rock failure, researchers can better understand the caving of the massive main roof, the compaction and load acquisition of the gob, the failure of the floor, and the stress redistribution in the coalbed and surrounding strata. With this knowledge, mines can be better designed to reduce dangerous bump occurrences.

Throughout the first two years of this project, a microseismic system was installed over a longwall district at a deep western coal mine. The overburden at this mine reaches 900 m (3,000 ft) and the lithology contains several notably competent units. In particular, the 180 m (600 ft) thick Castlegate sandstone, known for forming vertical cliffs in the surrounding escarpments, is approximately 165 m (550 ft) above the coal seam. The coal bed at the mine ranges from 2.4 to 6.0 m (8 to 20 ft) in thickness with an extraction thickness of 2.4 to 3.0 m (8 to 10 ft), and the geology immediately surrounding the seam consists of thinner (< 3 m (10 ft)) layers of siltstones, mudstones, shales, sandstones and coal.

The microseismic system at the mine consists of 23 geophones surrounding the coal mine both underground and on the surface. At present, the underground seismic array consists of 14 geophones in the mains and bleeders around the longwall panels (figure 9). On the surface over the mine, another nine geophones are distributed above the panels. At the mine office, a data analysis workstation receives the data from both the underground and surface geophones. These data are automatically analyzed in order to calculate the event locations, and then the locations are displayed in relation to a mine map on the computer screen for use by mine personnel.

At the time this paper was written, some 7,500 seismic events had been recorded from the first three quarters of panel 2. As an initial step in analyzing this information, the locations of the events were normalized to the advancing longwall face. The results of this normalization are shown in plan view in figure 10 and in a cross section parallel to the advance direction in figure 11. This is only preliminary data and the reader should understand that the exact location of these events may change in the future as the location algorithm is optimized based on field calibration data; however, the relative location of the events will remain fairly consistent and can be used at this time for some initial inferences.

From figures 10 and 11, it can be seen that the seismic activity is generally well in front of the face. This matches seismic data from other sites (*7*) and is interpreted to be the shear failure of the strata due to the forward stress abutment zone. From the plan view (figure 10), the seismic activity can be seen to curve back over the gateroads with a little more seismic activity located over the tailgate pillars than the headgate pillars. This result is consistent with strata failure above and below the yielding gateroad pillars, with the increased activity around the tailgate pillars due to the side abutment stress. From the side view (figure 11), it can be seen that the seismic activity is occurring both above and below the seam level. This response matches other field sites and is consistent with a front abutment that is vertically symmetric about the coal seam. Also, in figure 11, a slight angle (from vertical) of the seismic events back into the gob above the panel can be seen. This type of angle would be expected with the arching of the principal stress over the caved area in the gob.

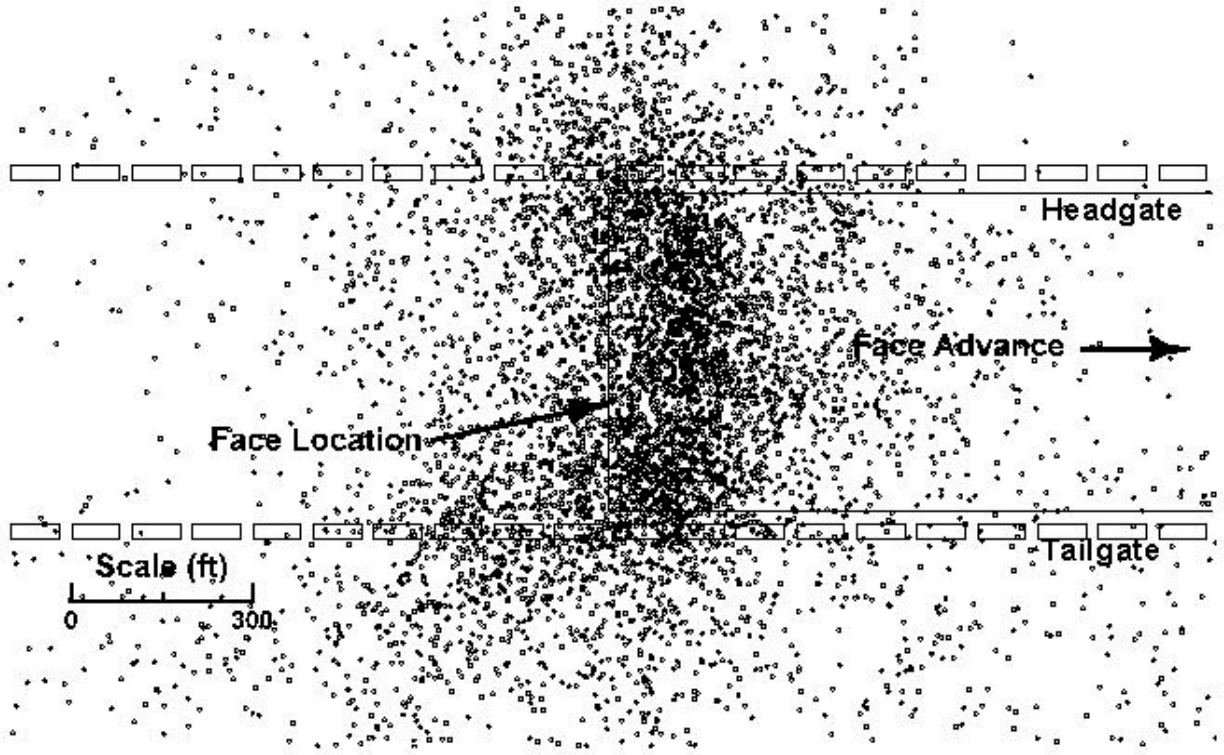


Figure 10. Plan view of event locations, normalized to face location

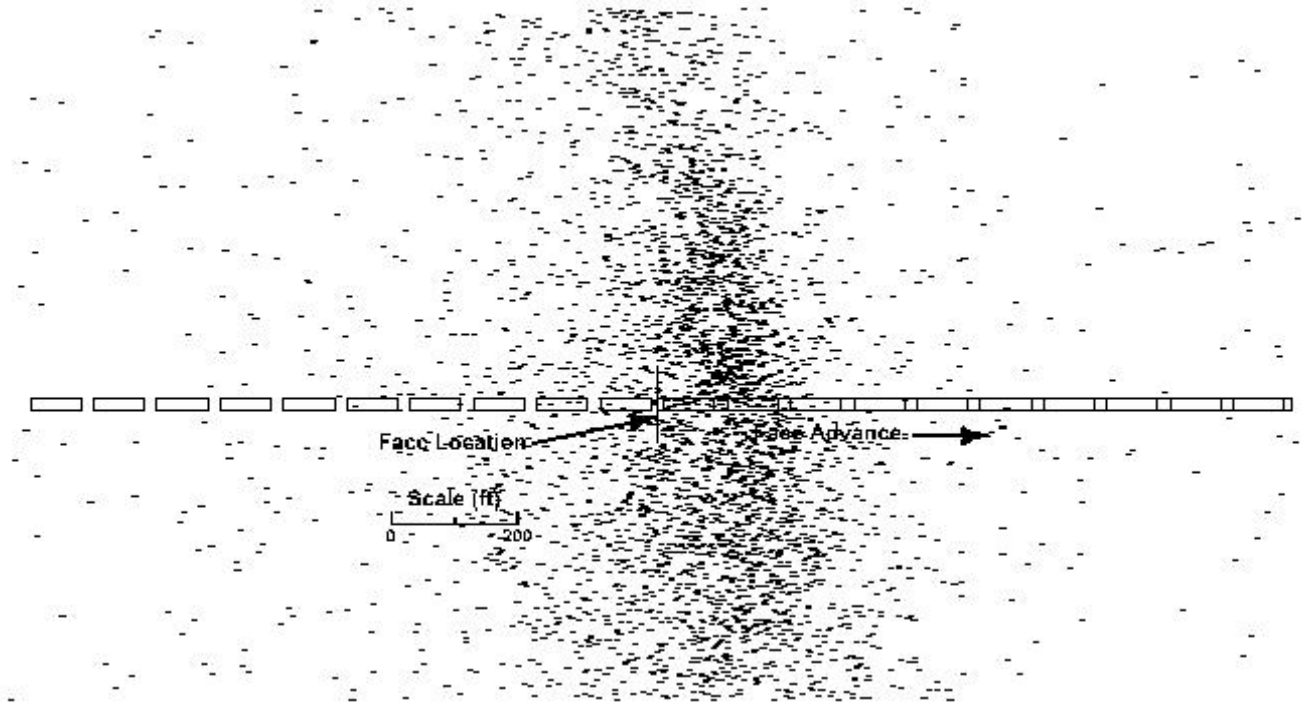


Figure 11. Cross sectional view of event locations, normalized to face locations

## REFERENCES


1. Rice GS. Bumps in Coal Mines of the Cumberland Field, Kentucky and Virginia-Causes and Remedy. U.S. Bureau of Mines RI 3267, 1935, 36 pp.
2. Iannacchione AT, Zelanko JC. Occurrence and Remediation of Coal Mine Bumps: A Historical Review. Paper in Proceedings: Mechanics and Mitigation of Violent Failure in Coal and Hard-Rock Mines. U.S. Bureau of Mines Spec. Publ. 01-95, 1995, pp. 27-67.
3. Zelanko JC, Heasley KA. Evolution of Conventional Gate-Entry Design for Longwall Bump Control: Two Southern Appalachian Case Studies. Paper in Proceedings of the Mechanics and Mitigation of Violent Failure in Coal and Hard-Rock Mines. U.S. Bureau of Mines Spec. Publ. 01-95, 1995, pp. 167-180.
4. Arabasz WJ, Nava SJ, Phelps TW. Mining Seismicity in the Wasatch Plateau and Book Cliffs Coal Mining Districts, Utah, USA-Overview and Update. Proceedings of the 15th International Conference on Ground Control in Mining, Golden, CO, August 13-15, 1996, 28 pp.
5. Mark C. Pillar Design Methods for Longwall Mining, U.S. Bureau of Mines IC 9247, 1990, 53 pp.
6. Kanamori, H., J. Mori, E. Hauksson, T. Heaton, L. K. Hutton, and L. M. Jones. Determination of Earthquake Energy Release and ML Using Terrascope. Bull. Seis. Soc. Am. No. 83, 1993, pp. 330-346.
7. Hatherly P, Lou X, Dixon R, McKavanagh B, Berry M, Jecny Z, Bugden C. Roof and Goaf Monitoring for Strata Control in Longwall Mining. Final Report ACARP C3067, 1995.